CENP-E forms a link between attachment of spindle microtubules to kinetochores and the mitotic checkpoint

Xuebiao Yao*†, Ariane Abrieu†, Yun Zheng*, Kevin F. Sullivan§ and Don W. Cleveland†‡¶

*Department of Physiology, University of Wisconsin, Madison, Wisconsin 53706, USA
†Ludwig Institute for Cancer Research, University of California at San Diego, 9500 Gilman Drive, La Jolla, California 92093-0660, USA
‡Departments of Medicine and Neuroscience, University of California at San Diego, 9500 Gilman Drive, La Jolla, California 92093-0660, USA
§Department of Cell Biology, Scripps Research Institute, 10550 North Torrey Pines Road, La Jolla, California 92037, USA
¶e-mail: dcleveland@ucsd.edu

Here we show that suppression of synthesis of the microtubule motor CENP-E (centromere-associated protein E), a component of the kinetochore corona fibres of mammalian centromeres, yields chromosomes that are chronically mono-orientated, with spindles that are flattened along the plane of the substrate. Despite apparently normal microtubule numbers and the continued presence at kinetochores of other microtubule motors, spindle poles fragment in the absence of CENP-E, which implicates this protein in delivery of components from kinetochores to poles. CENP-E represents a link between attachment of spindle microtubules and the mitotic checkpoint signalling cascade, as depletion of this motor leads to profound checkpoint activation, whereas immunoprecipitation reveals a nearly stoichiometric association of CENP-E with the checkpoint kinase BubR1 during mitosis.

Chromosome movements during mitosis are orchestrated primarily by the interaction of spindle microtubules with the kinetochore[1], the site for attachment of spindle microtubules to the centromere. In addition to providing a physical link between chromosomes and spindle microtubules, the kinetochore has an active function in chromosomal segregation through microtubule motors located at or near it[2–4]. In the typical mammalian case, early prometaphase involves the capture of a microtubule by one of the two kinetochores of a duplicated chromosome pair and subsequent transport of the microtubule towards the corresponding pole. As it nears the pole its movement becomes oscillatory, moving towards and away from the pole[5–7], until the unattached kinetochore of the mono-orientated chromosome pair finally captures a microtubule from the opposite pole. This initiates congression of chromosomes to the spindle equator in a series of a discontinuous movements that are also characterized by directional switching[8]. Laser-dissection experiments have shown that most of the force for chromosome congression arises at the leading kinetochore[9]. Despite these findings, the kinetochore components that are responsible for microtubule capture, generation of kinetochore-dependent forces for powering chromosome movement, and the mechanism(s) responsible for balancing the net force to produce congression, as well as the subsequent chromosome movement in anaphase, remain unidentified.

Several lines of evidence have implicated the kinetochore in generation of a diffusible checkpoint signal that can block cell-cycle progression into anaphase until all kinetochores have successfully attached to spindle microtubules. Delayed attachment of one or more chromosomes to the spindle is correlated with a corresponding delay in the onset of anaphase[10]. Genetic analyses of yeast[11,12], micromanipulation experiments with insect spermatocytes[13,14] and laser-ablation studies in mammalian cells[10] have led to the conclusion that the inhibitory checkpoint signal arises either from unattached or improperly attached kinetochores, or from absence of tension arising from opposing forces generated at sister kinetochores. Three MAD (mitotic arrest deficiency)[13] and three BUB (budding uninhibited by benomyl)[12] genes have been identified in budding yeast that fail to arrest the cell cycle in mitosis after drug-induced microtubule disassembly. Vertebrate homologues of Mad2 (refs 15, 16), BUB3 (refs 17, 18), Bub1 (ref. 19) and BubR1 (related to both BUB1 and Mad3; ref. 17), are transient kinetochore components. Expression of the kinetochore-binding domain of murine BUB1 (ref. 19) or injection of antibodies against BubR1 (ref. 20) results in premature onset of anaphase, presumably by replacement of the endogenous proteins at kinetochores. Collectively, these data indicate that binding of these spindle checkpoint components to unattached kinetochores may generate a signal that is produced at, and then released from, kinetochores.

Cell-cycle-dependent accumulation of CENP-E[21] yields a maximum of ~5000 molecules per HeLa cell at the G2/M-phase transition (that is, about 50 molecules per kinetochore[22]). The following findings indicate that altering its action can affect chromosome movements: first, antibodies against CENP-E inhibit poleward chromosome movements powered by microtubule disassembly *in vitro*[23]; second, injection of antibodies into cells slows down the metaphase-to-anaphase transition[24]; third, injection of antibodies into mouse eggs completely blocks meiosis I at the prometaphase/metaphase transition[25]; fourth, injection of antibodies into mammalian cells prevents chromosome alignment and causes chromosomes to oscillate between spindles[26]; and fifth, immunodepletion of CENP-E from *Xenopus* egg extracts disrupts chromosome congression[21]. Along with proof that a motor-containing fragment of CENP-E can use ATP to power movement toward microtubule plus ends *in vitro*[21], this evidence indicates that CENP-E may function as a kinetochore-associated microtubule-binding component and as a motor. CENP-E has also been implicated as a binding partner for the mitotic-checkpoint kinase BubR1 (refs 20, 27).

Here we investigate the function of CENP-E in attachment of kinetochores to spindle microtubules, alignment of chromosomes, and checkpoint signalling, using antisense oligonucleotides to suppress its synthesis and accumulation. We show that CENP-E is essential for stable, bi-orientated attachment of chromosomes to spindle microtubules, for development of tension across aligned chromosomes, for stabilization of spindle poles and for satisfying the mitotic checkpoint.

Results

Antisense-mediated reduction in CENP-E levels. To investigate the influence of CENP-E on attachment of chromosomes to spindle

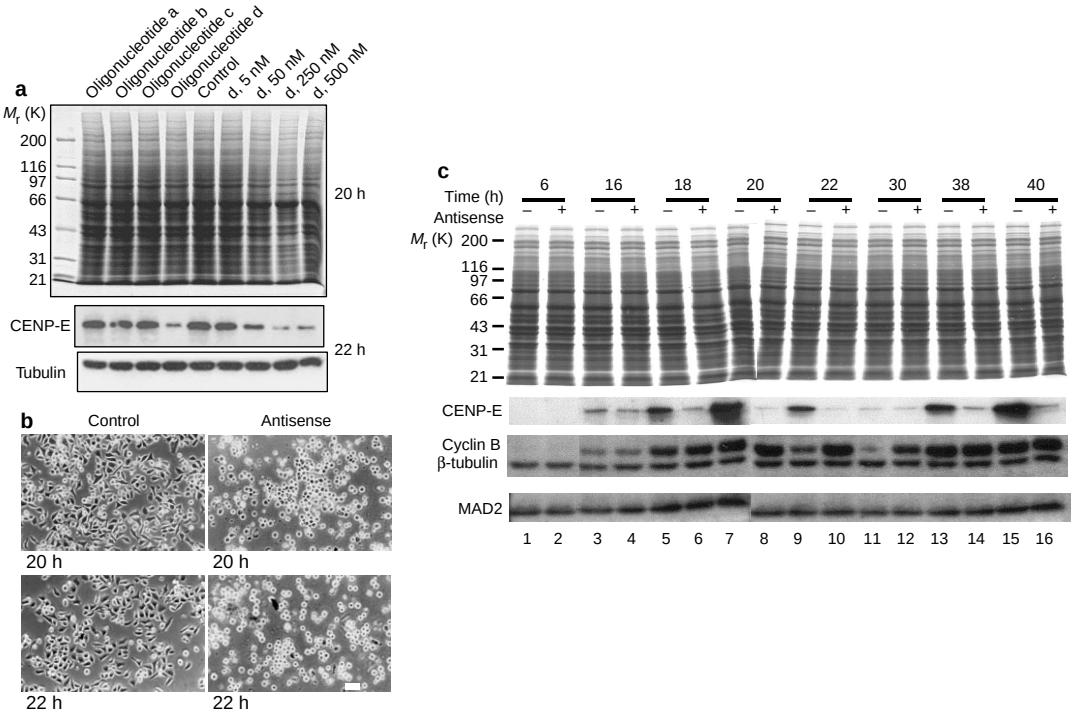

Figure 1 **Antisense suppression of CENP-E induces long-term mitotic arrest.** **a**, Mitotic HeLa cells were transfected with the indicated oligonucleotides (oligonucleotide d at the indicated concentrations) and subjected to SDS–PAGE and immunoblotting. Upper panel, Coomassie-stained proteins. Middle and lower panels, immunoblots against CENP-E (middle) and tubulin (lower). **b**, Phase-contrast images of control cells and cells treated with CENP-E antisense oligonucleotide d. Images were obtained at the indicated times after transfection. Scale bar represents 30 μm. **c**, Levels of CENP-E, cycling B, tubulin and Mad2, in cells transfected with control (–) antisense (+) oligonucleotides, at the indicated times after transfection, as shown by SDS–PAGE and immunoblotting.

microtubules and on the mechanism of mitotic-checkpoint signalling, we introduced a series of antisense oligonucleotides to CENP-E by transfection into HeLa cells synchronized by mitotic shake-off to be in the early G1 phase of the cell cycle. As CENP-E protein is nearly quantitatively degraded at the end of mitosis[22], suppression of new synthesis in early G1 cells allowed us to examine CENP-E function without the complication of a pre-existing pool of CENP-E.

To determine the efficiency of inhibition of CENP-E accumulation, we collected cells after 20 h, at which time control cells and those transfected with a scrambled antisense oligonucleotide had cycled to the next mitosis and had accumulated maximal levels of CENP-E. Immunoblotting with an antibody against CENP-E revealed that whereas three initial oligonucleotides (oligonucleotides a–c, Fig. 1a) failed to significantly suppress CENP-E levels, 250 nM (or greater) of oligonucleotide d, an 18-mer centered on the ATG translation-initiation codon of CENP-E, caused an eightfold reduction of CENP-E levels without altering the levels of other proteins such as tubulin. Cells transfected with oligonucleotide d covalently attached to fluorescein exhibited a comparable level of inhibition, and examination by fluorescence microscopy proved that in different transfections, 81–89% of cells contained measurable levels of oligonucleotide. As CENP-E synthesis in the ~11–19% of cells with little or no oligonucleotide was unlikely to be markedly diminished, the observed eightfold inhibition must represent almost complete inhibition of CENP-E in 85±4% of successfully transfected cells.

Suppression of CENP-E causes mitotic arrest with high levels of cyclin B. To examine the effect of suppression of CENP-E on cell-cycle progression, we obtained cells by mitotic shake-off, transfected them with 250 nM oligonucleotide d and examined them by phase-contrast microscopy at regular time intervals. In cells with normal CENP-E levels (transfected with an oligonucleotide of the same nucleotide composition as oligonucleotide d but with a scrambled sequence), a wave of mitosis was seen; a peak was observed at 20 h, at which time 61% of cells were in mitosis, as scored by the number of rounded cells (Fig. 1b) and confirmed by the absence of intact nuclei under DAPI staining (data not shown). In contrast, although cells with diminished CENP-E levels proceeded through interphase with roughly the same cell-cycle time, they retained a rounded conformation (Fig. 1b) that was indicative of mitotic arrest. At 20 h the mitotic index was 81% and thereafter remained at a high level (79% at 22 h, Table 1), which is consistent with almost total mitotic arrest in the transfected cell population. Staining with vital dyes demonstrated the continuing viability of arrested cells, and staining with DAPI showed that mitotic chromosome morphology was maintained for at least the duration of an entire cell cycle (20 h, as shown by the second wave of mitosis in the control cell population).

To confirm the successful reduction in levels of CENP-E during progression through interphase and subsequent mitotic arrest, we collected aliquots of cells transfected with the CENP-E antisense

Table 1 Loss of CENP-E causes mitotic arrest

Mitotic Index*		
Time after treatment	20 h	22 h
Control	61%	19%
Antisense-treated	81%	79%

* Mitotic cells were defined by the absence of a nuclear envelope and the presence of condensed chromosomes. Mitotic index is expressed as the percentage of the total cell population that in mitosis at the indicated time point. Data were obtained from >250 cells in 5 different fields.

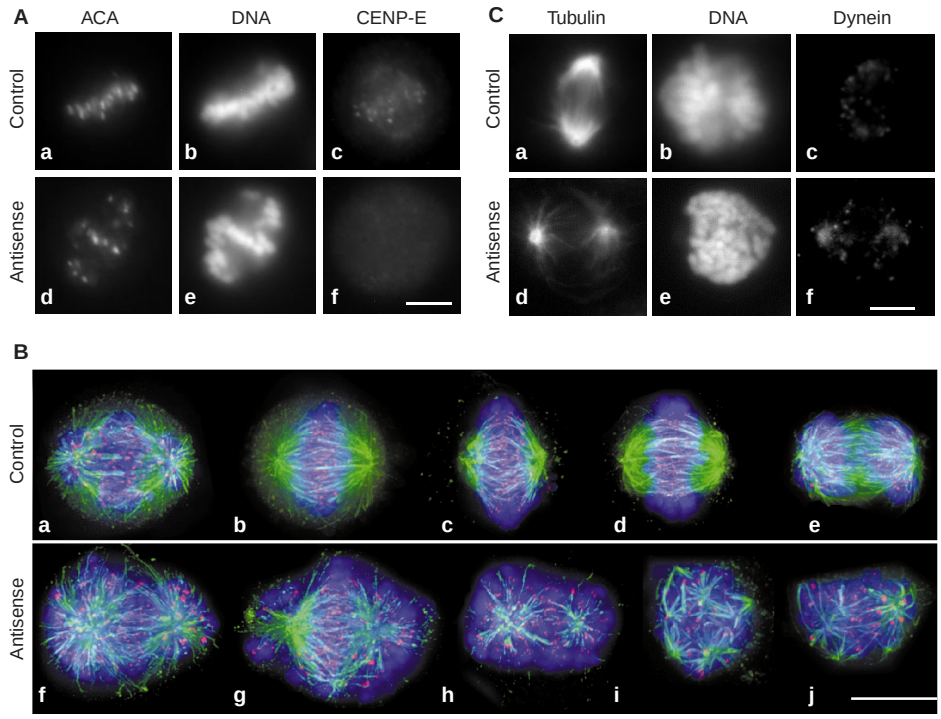

Figure 2 **Loss of CENP-E does not affect spindle assembly, but causes chromosome misalignment. A**, Loss of CENP-E affects chromosome congression to the spindle equator. Indirect immunofluorescence images of HeLa cells treated with control (**a–c**) or antisense (**d–f**) oligonucleotides. Cells were stained with ACA (**a**, **d**), DAPI (**b**, **e**), and anti-CENP-E antibody (**c**, **f**). Scale bar represents 10 μm. **B**, Deconvolution images of mitotic HeLa cells 22 h after transfection with a scrambled oligonucleotide (**a–e**) or with CENP-E antisense oligonucleotide d (**f–j**). Cells were stained with CREST antisera (red), DAPI (blue) and anti-tubulin antibody (green). Scale bar represents 10 μm. **C**, Indirect immunofluorescence images of HeLa cells treated with control (**a–c**) or antisense (**d–f**) oligonucleotides. Cells were stained with anti-tubulin antisera (**a**, **d**), DAPI (**b**, **e**) and with an antibody against cytoplasmic dynein (**c**, **f**). Scale bar represents 10 μm.

oligonucleotide d or with the scrambled control oligonucleotide, at varying time intervals for 40 h after transfection. As expected, no CENP-E was detected early in interphase in either antisense-treated or control cells (Fig. 1c, lanes 1 and 2). CENP-E levels remained consistently low at all subsequent times in antisense-transfected cells, whereas in control cells CENP-E levels exhibited the expected cyclicity, increasing 15-fold by 20 h before becoming almost undetectable by 30 h and then rising again as the cell population approached a second mitosis at 38–40 h (Fig. 1c). We confirmed this by monitoring cyclin B levels — after 20 h of suppression of CENP-E, cyclin B levels had risen to levels that were comparable to those in control cells; however, these high cyclin B levels continued for up to 40 h in cells with diminished CENP-E (Fig. 1c, lane 16). Levels of both tubulin and of the other principal cell polypeptides visible by staining with Coomassie blue showed no fluctuations in antisensed cells, which demonstrates further the specificity of the suppression of CENP-E synthesis (Fig. 1c). The reduction in total CENP-E content was also reflected in loss of CENP-E at kinetochores, as demonstrated by double indirect immunofluorescence with antibodies against CENP-E (Fig. 2A, compare c and f), whereas levels of other centromere antigens (recognized by CREST anticentromere antisera (ACA)) were unaffected (Fig. 2A, compare a and d).

Thus, absence of CENP-E does not affect progression through interphase, but does cause an almost complete long-term mitotic arrest.

Absence of CENP-E yields flattened bipolar spindles and misaligned chromosomes. To determine whether the prometaphase arrest that arises from elimination of CENP-E reflects an underlying defect in spindle assembly or maintenance, we visualized spindles with antibodies against tubulin and identified centromeres with ACA. As expected, synchronized control cells passing through the initial mitotic wave were observed in all phases of the mitotic cycle (including early and late prometaphase, metaphase, and early and late anaphase; Fig. 2Ba–e, respectively). In contrast, at comparable time points, most CENP-E antisense-treated cells had established bipolar spindles but each contained lagging chromosomes that were readily apparent (Fig. 2A, d, and B, f–h). Examination of ~100 mitotic cells blocked by antisense revealed that many chromosomes in almost all (83%) antisense-treated cells were positioned close to spindle poles, with a few apparently bi-orientated at or near to the spindle equator (Fig. 2B, f–j) and fewer still at intermediate positions. This pattern is the expected distribution for chromosomes that are actively congressing. The pattern of misaligned chromosomes did not change in a 30-h period of prolonged mitotic arrest in CENP-E-depleted cells. Spindles in these cells were markedly flatter (4.2±1.75 μm, $n=15$) than those in control cells (8.3±2.4 μm, $n=7$). In addition, a minority of spindles in CENP-E-depleted cells exhibited apparent fragmentation of spindle poles,

Table 2 Elimination of CENP-E releases tension between sister kinetochores

Treatment	Distance (μm)*
Control	1.7±0.13
Antisense: aligned kinetochores	1.3±0.21
Antisense: misaligned kinetochores	1.2±0.14
Antisense: nocodazole-treated	1.0±0.10

* Distance between ACA-labelled sister kinetochores. Data were obtained from >100 kinetochore pairs in which both kinetochores were in the same focal plane (see Methods).

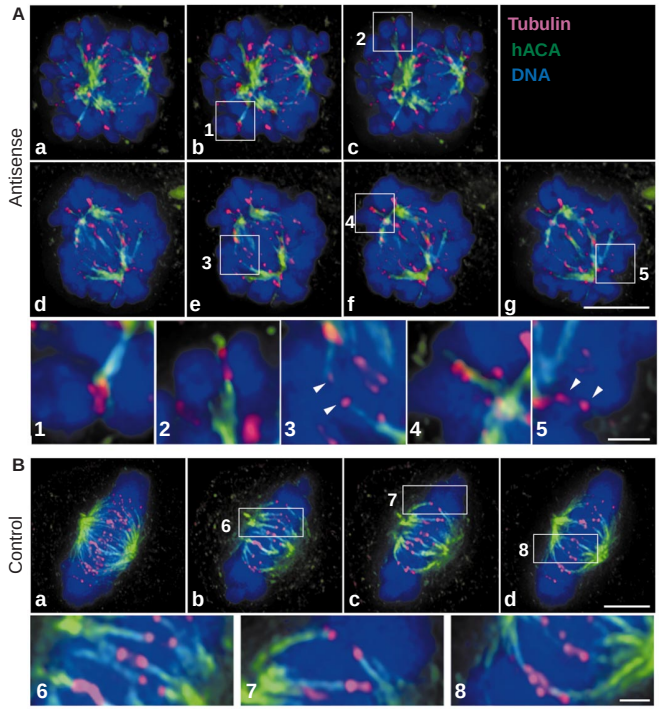

Figure 3 **Reduced capture or stability of kinetochore-associated microtubules in the absence of CENP-E. A**, Deconvolution-microscopic images of cells after antisense suppression of CENP-E. Images show immunofluorescence staining of ACA (red), DNA (blue) and tubulin (green). **a**, **d**, Image projections of sums of optical sections. **b**, **c**, **e–g**, Individual optical sections of the corresponding images **a** (**b, c**) or **d** (**e–g**). Insets show parts of these images. Arrows in inset 3 show a bi-orientated chromosome pair; arrows in inset 5 show a kinetochore pair without stable microtubule attachment. **B**, Deconvolution images of cells treated with control oligonucleotide. **a**, Sum of optical sections. **b–d**, Individual sections. Scale bars represent 10 μm (cell images) and 2 μm (insets).

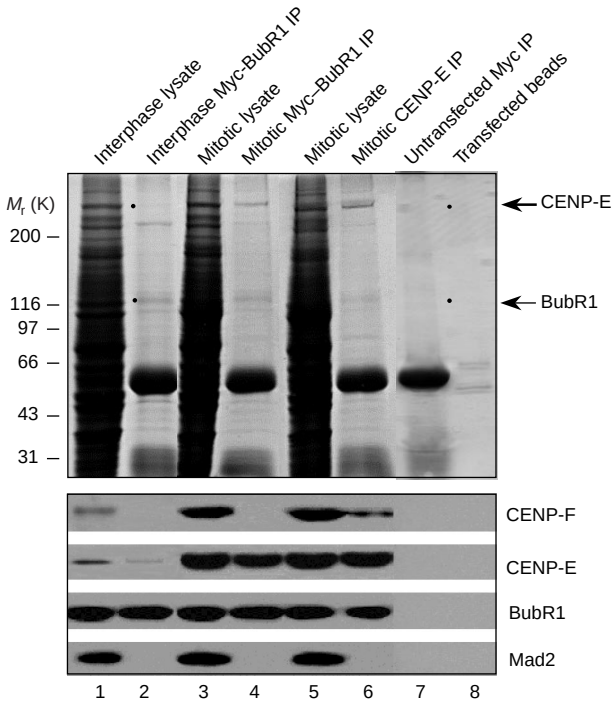

Figure 4 **Identification of CENP-E binding partners in normal cells.** Extracts from interphase (lanes 1, 2) or mitotic (lanes 3–6) HeLa cells expressing Myc-tagged BubR1 were incubated with antibodies against Myc antibody (lanes 2, 4) or CENP-E (lane 6) and immunoprecipitates (IP) were resolved by SDS–PAGE. Interphase cells were collected 16 h after mitotic shake-off. Mitotic cells were obtained after 16 h of culture in nocodazole. Lane 7, immunoprecipitation with anti-Myc antibody from extracts of untransfected cells. Lane 8, immunoprecipitation from transfected cells with protein-A beads only. Upper panel, Coomassie-stained proteins. Twice the proportion of each immunoprecipitate, compared with the initial amount of cell lysate, was analysed to enhance observation of protein profiles. Lower panel, immunoblotting with antibodies against CENP-F, CENP-E, the Myc epitope tag on BubR1, and Mad2.

producing multipolar arrays and a higher proportion of unattached chromosomes (Fig. 2B, i and j).

Absence of CENP-E reduces tension at kinetochores of bi-orientated chromosomes. As the interkinetochore distance on sister chromatids has previously been proposed as an accurate reporter for judging tension developed across the kinetochore pair[28], we measured this distance in >100 kinetochore pairs in which both kinetochores were in the same focal plane, in both CENP-E-depleted and control cells (Table 2). Control kinetochores exhibited a separation of 1.7±0.1 μm, whereas the distance between apparently aligned kinetochores in antisense-treated cells was 1.3±0.2 μm. The interkinetochore distance of misaligned kinetochores in antisense-treated cells was 1.2±0.1 μm, whereas this distance in nocodazole-treated cells, in which kinetochore pairs were presumably under no tension, was 1.0±0.1 μm. We conclude that reduced levels of kinetochore-associated CENP-E give rise to kinetochores that are under much less tension.

In addition to CENP-E, two other proteins, cytoplasmic dynein[29,30] and mitotic-centromere-associated kinesin (MCAK)[31] have been implicated as microtubule-dependent motors that function at or near to kinetochores. In early prometaphase in CENP-E containing cells, dynein was associated with kinetochores, as reported previously[29,30] (Fig. 2C, c). Elimination of CENP-E by antisense treatment did not affect cytoplasmic dynein, which continued to exhibit apparent centromere localization (Fig. 2C, f) and was occasionally localized along the spindle microtubules. In the absence of CENP-E, the intensity of kinetochore labelling by dynein was consistently higher, indicating that CENP-E may reduce kinetochore–dynein affinity or the number of dynein-binding sites on the kinetochore. Association of MCAK with the kinetochore was not affected by suppression of CENP-E (data not shown).

Absence of CENP-E diminishes stable microtubule binding at kinetochores. To investigate how the absence of CENP-E, which is known to extend at least 50 nm from the kinetochore surface[32], affects the attachment and stability of spindle microtubules to kinetochores, we preferentially disassembled most of the labile, non-kinetochore-associated microtubules by brief exposure to low temperature, as described previously[33,34]. We briefly chilled control and CENP-E antisense-treated cells to 4 °C; they were then extracted, fixed and stained with anti-tubulin antibody and ACA. As expected, most non-kinetochore-associated microtubules were lost, but images obtained by optical sectioning with deconvolution microscopy showed that centromeres labelled by ACA remained associated with spindle microtubule ends in control cells (Fig. 3B, red dots). In CENP-E-depleted cells, a few chromosomes were aligned and bi-orientated (Fig. 3A, inset 3), with kinetochore fibres that showed little or no diminution in the apparent number of associated microtubules (as determined by fluorescence intensity) compared with those of control cells.

A complete series of optical sections revealed that most kinetochores of chromosomes that were scattered around the poles did not establish or maintain bipolar attachments (Fig. 3A, insets 1 and

4); this was true of many kinetochores without stable microtubule fibres (Fig. 3A, inset 5). Unexpectedly, we also found several examples in which both kinetochores seemed to be attached to microtubule bundles, but one set of fibres appeared to have fragmented or detached from the more distal pole (Fig. 3A, inset 2) or in which both kinetochores were apparently attached to the same microtubule bundle (Fig. 3A, inset 4). Although cold-resistant attachment of kinetochores to spindle microtubules can thus be achieved for a subset of chromosomes when CENP-E levels are diminished, the abundance of chromosomes without stable bipolar attachments even after long periods of mitotic arrest firmly indicates that CENP-E must have an important function in the initial capture and/or subsequent stabilization of microtubules. Thus, the failure of stable bi-orientated attachment and subsequent chromosome congression to occur is a specific consequence of reduction in CENP-E.

CENP-E forms a complex with the mitotic-checkpoint component BubR1. A direct interaction between CENP-E and BubR1, a component that is implicated in checkpoint signalling by virtue of its sequence similarity to both *Saccharomyces cerevisiae* Bub1 and Mad3 (ref. 17), has previously been proposed on the basis of interactions observed in yeast two-hybrid assays between the kinetochore-binding portion of CENP-E and BubR1 (refs 20, 27). To test for such an interaction, we used anti-CENP-E antibodies to immunoprecipitate soluble CENP-E and potential partner proteins from lysates of mitotically arrested HeLa cells transiently transfected to express epitope-tagged BubR1. Coomassie staining of the immunoprecipitate showed that it contained, in addition to the antibody heavy (relative molecular mass 55,000 (M_r55K)) and light (M_r25K) chains, both CENP-E (M_r >300K) and a roughly stoichiometric amount of another polypeptide (estimated M_r110K; Fig. 4, lane 6). Immunoblotting with anti-CENP-E antibody confirmed the M_r >300K polypeptide to be CENP-E, and immunoblotting against the epitope tag demonstrated that the M_r110K species was BubR1 (Fig. 4, lane 3).

Immunoprecipitation of BubR1 using an antibody against the epitope tag confirmed the presence of a complex of BubR1 and CENP-E, although the proportion of BubR1 relative to CENP-E in the precipiate (Fig. 4, lane 4) was 3–5 times that seen with anti-CENP-E antibodies (Fig. 4, lane 6), which is consistent with a greater accumulation of tagged BubR1. No M_r110K polypeptide was precipitated with the anti-epitope-tag antibody from extracts of untransfected cells (Fig. 4, lane 7) or with protein-A beads alone (Fig. 4, lane 8). We tested further the specificity of the BubR1–CENP-E complex by immunoprecipitating it from extracts of interphase cells, which naturally contain greatly reduced levels of CENP-E (Fig. 4, lane 1). A comparable level of BubR1 was precipitated with the anti-epitope-tag antibody, but only a trace amount of co-precipitated CENP-E was observed (Fig. 4, lane 2).

We tested for the presence of other known kinetochore proteins in CENP-E immunoprecipitates by immunoblotting similar precipitates with a range of other antibodies. No Mad2 was detected in any of the immunoprecipitates, but a small proportion of CENP-F, which has been proposed to be a potential binding partner for CENP-E[27], was consistently co-precipitated from mitotic extracts (Fig. 4, lane 6).

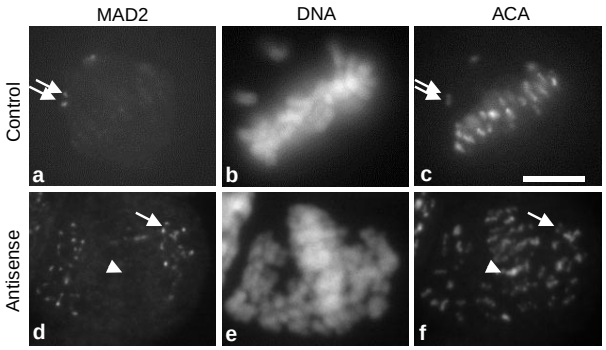

Figure 5 **Suppression of CENP-E results in failure to silence the mitotic checkpoint.** Immunofluorescence staining of the checkpoint protein Mad2 (**a**, **d**), the centromere marker ACA (**c**, **f**) and DNA (**b**, **e**) in control (**a–c**) and CENP-E-antisensed (**d–f**) cells. Arrowheads show chromosome pairs with unresolved centromeres in ACA; arrows show misaligned chromosomes retaining high levels of Mad2. In antisense-treated cells, Mad2 labelling is restricted to chromosomes scattered near the poles. Scale bar represents 10 μm.

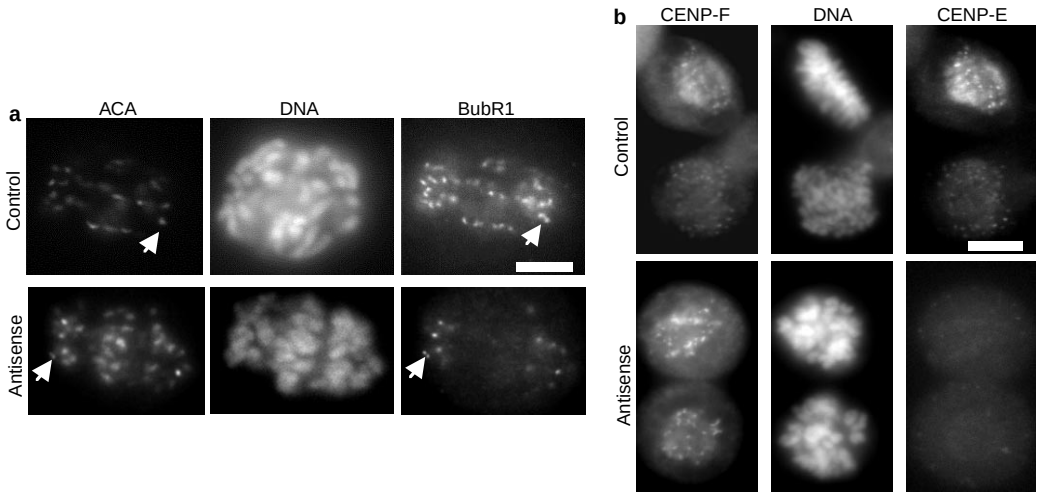

Figure 6 **CENP-E binding partners remain associated with the kinetochore in the absence of CENP-E. a**, Loss of BubR1 from centrally orientated, aligned chromosomes. Images show immunofluorescence staining of CREST ACA (left panels), BubR1 (right panels) and DNA (middle panels) in control prometaphase cells (upper panels) and in cells with reduced levels of CENP-E (lower panels). Arrows show examples of misaligned chromosome pairs near spindle poles. **b**, Localization of CENP-F to kinetochores is independent of CENP-E. Images show immunofluorescence staining of CENP-F (left panels), CENP-E (right panels) and DNA (middle panels) in control (upper panels) and antisense-treated (lower panels) cells. Scale bars represent 10 μm.

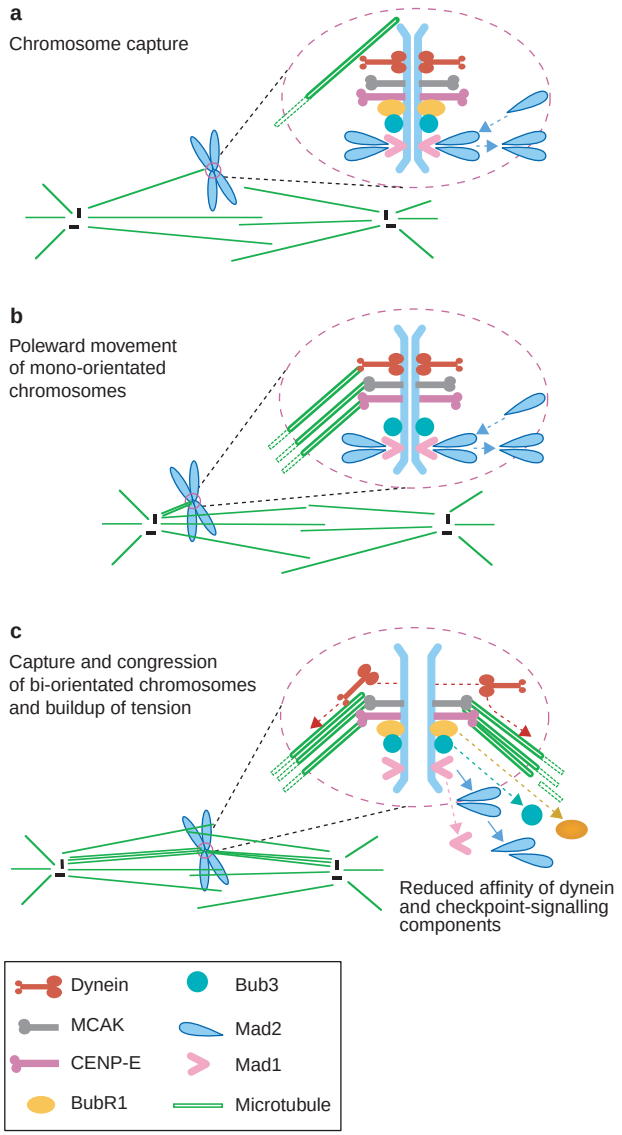

Figure 7 **Model for the mitosis-related functions of CENP-E.** In this model, cytoplasmic dynein (or an unidentified minus-end directed motor) mediates initial lateral attachment of mono-orientated chromosomes to spindle microtubules and rapid translocation of chromosomes to the adjacent pole. CENP-E is required for efficient, stable capture by the previously unoccupied kinetochore and for successful congression or maintenance of congression to a mitotic midzone. Development of normal levels of tension across bi-orientated kinetochore pairs, as reflected in the spatial separation of sister kinetochores, requires CENP-E tethering and/or motor activity. The effect of increased occupation of microtubules by CENP-E and/or increased deformation through tension is twofold. First, BubR1 (a checkpoint kinase that is bound to CENP-E when the checkpoint is signalling) and Bub3 (ref. 18) are partially released, and second, formation at kinetochores of an activated form of Mad2 (shown as a Mad2 dimer[48]) is blocked, preventing inhibition of the ubiquitin-ligase activity of the anaphase-promoting complex (APC).

Normal levels of CENP-E are required for mitotic-checkpoint signalling. Mitotic-checkpoint signalling in mammalian mitosis is normally activated immediately after disassembly of the nuclear envelope, as unattached chromosomes spill into the cytoplasm[10,15,18]. To determine whether the checkpoint remains activated during the long-term arrest provoked by elimination of CENP-E, we used triple immunofluorescence to localize the checkpoint component Mad2 (ref. 11) to chromosomes after CENP-E depletion. Mad2 has been shown to bind preferentially to unattached kinetochores[15,16] or to those that are attached but not under tension[13], but to release as (or just after) bipolar attachments are formed and tension is increased across the bi-orientated chromosomes. Consistent with continued activation of the mitotic checkpoint from misaligned chromosomes, high levels of kinetochore-associated Mad2 remained on lagging chromosomes (Fig. 5a, d, arrows) but not on chromosomes near the spindle equator (Fig. 5a, d, arrowheads). As expected, aligned chromosomes in control metaphase cells showed no kinetochore-associated Mad2. The retention of Mad2 binding to kinetochores on lagging chromosomes indicates that CENP-E function is necessary for silencing spindle-checkpoint signalling from misaligned chromosomes.

To investigate the effect of CENP-E suppression on the localization of BubR1 or CENP-F at kinetochores, we determined the positioning of each of these components in cells lacking CENP-E. As expected, BubR1 in control cells in early prometaphase was found at the centromeres of most chromosomes (Fig. 6a, upper-right panel, arrow); by late prometaphase it was present at reduced levels on fully congressed chromosomes (data not shown). In antisense-treated cells, BubR1 remained associated with the kinetochores of misaligned chromosomes (such as those close to either spindle pole; Fig. 6a, lower-right panel, arrow), but its staining intensity was markedly reduced on chromosomes that were centrally positioned and presumably bi-orientated (Fig. 6a, lower-right panel). Continued kinetochore localization after CENP-E suppression was also seen for CENP-F (Fig. 6B, f). We conclude that localization of CENP-F and BubR1 to kinetochores is independent of CENP-E and that both binding of BubR1 to unattached chromosomes and its release from aligned chromosomes can be achieved in the absence of normal levels of its partner protein CENP-E, which is consistent with the finding that an injected anti-CENP-E antibody displaces CENP-E from kinetochores without affecting the kinetochore localization of BubR1 (ref. 20).

Discussion

We have shown that in the absence of CENP-E cells remain in mitosis for extended periods, fail to establish stable bipolar attachments to chromosomes and develop abnormally flat spindles. The failure of stable bipolar attachment strongly indicates that CENP-E functions in one or more steps of the centromere–microtubule interaction, including initial capture and microtubule stabilization or formation of mature attachments. This reinforces and extends three previous lines of evidence. First, chromosome movement *in vitro*, powered by disassembly of a kinetochore microtubule, is blocked by antibodies against CENP-E, but not by antibodies against other kinetochore motors[23]; second, chromosome alignment is either not established or not maintained in spindles assembled *in vitro* after removal of CENP-E[21]; and third, chromosomes do not congress in cultured cells injected with anti-CENP-E antibodies[26]. Together, these findings indicate that CENP-E must be a critical linking factor that mediates stability of spindle microtubules at kinetochores and/or linkage of kinetochore bundles to the bulk microtubules of the spindle without affecting the number of microtubules bound. The other lines of evidence mentioned above are as follows: However, it is uncertain whether the bi-orientated chromosomes seen in CENP-E-depleted cells had undergone congression from a peripheral position, or had initially condensed in a central position, captured polar microtubules and remained in a central location. Despite their resistance to cold-induced microtubule disassembly, it is also unknown whether microtubule bundles attached either to mono-orientated or bi-orientated chromosomes really have lifetimes that are comparable to those of typical kinetochore fibres, or whether the absence of CENP-E generates unstable kinetochore

fibres, producing chromosomes that cycle between mono- and bi-orientation.

Although chromosome-positioning abnormalities were not unexpected, elimination of CENP-E revealed that this motor protein contributes to the geometry and stability of bipolar spindles. Spindles in CENP-E-depleted cells were markedly flatter and spindle poles were frequently fragmented, effects that were not previously identified by antibody injection[26] or by transfection of cells with the CENP-E kinetochore-targeting domain[27]. Although flattening of the spindle may simply be a consequence of reduced tension between the poles (a consequence of the reduction in the number of stable bipolar attachments and in the tension applied across those chromosomes), a further factor may be the apparent increase in the amount of kinetochore-bound cytoplasmic dynein in the absence of CENP-E. This indicates not only that the two motors may compete for a common or overlapping set of kinetochore-binding sites, but also that CENP-E may be required for appropriate release of dynein and its mitotic cargoes, including ZW10 (ref. 35) and NuMA[36]. Reduced delivery (or maintenance of delivery) of the latter would fully account for the observed fragmentation of the spindle pole, as dynein-mediated delivery of a dynein–dynactin–NuMA complex is required for tethering of polar microtubules to each other and to the centrosome[36,37].

Whatever the case, the establishment of many monopolar and some bipolar attachments in CENP-E-depleted spindles supports the idea that CENP-E itself is not uniquely required for attachment of spindle microtubules to kinetochores. Rather, two other mitotic motor proteins that localize within the kinetochore, cytoplasmic dynein[29,30] and MCAK/XKCM1 (refs 31, 38), are candidates for the basal attachment seen in CENP-E-depleted cells (modelled in Fig. 7). For MCAK/XKCM1, there is no direct evidence of kinetochore-tethering activity. Rather, the *Xenopus* homologue XKCM1 is a potent microtubule destabilizer that is targeted to microtubule ends *in vitro* and promotes microtubule castastrophe[39]. Antisense suppression of the mammalian homologue (MCAK) gives rise to lagging chromosomes in anaphase, without apparently affecting chromosome attachment or congression[40]. A dynein-like, minus-end-directed motor is clearly involved in initial lateral attachment of microtubules to kinetochores[3]. However, microinjection of antibodies against dynein[41] or disruption of the dynein activator dynactin[42] results in spindle collapse, rather than a direct effect on chromosome attachment to spindles. The simplest view is that either CENP-E or cytoplasmic dynein can form initial mono-orientated linkage of centromeres to spindle microtubules (Fig. 7), but that a combination is required to efficiently convert and stabilize these initial lateral interactions, forming the mature ones that allow active congression. This is all the more crucial for capture of microtubules by the second kinetochore of a chromosome pair (Fig. 7b), and CENP-E seems to have a key function in this process, as suppression of this protein produces chronic mono-orientation of many chromosomes.

Finally, what seems readily apparent is that, after initial activation of the mitotic checkpoint as the nuclear envelope is disassembled, one or more kinetochore-associated microtubule-binding components must be involved in linking microtubule attachment to checkpoint silencing. Indeed, suppression of CENP-E leads to chronic activation of the mitotic checkpoint (Fig. 1) and continued association of high levels of Mad2 and BubR1 with many misaligned kinetochores (Figs 5, 6). Although this many reflect indirect participation of CENP-E in checkpoint signalling through CENP-E-dependent stabilization of microtubule capture, the roughly stoichiometric nature of the mitotic complex of soluble CENP-E and kinetochore-associated kinase BubR1 (Fig. 4) indicates that CENP-E may have a more direct function. Combined with the loading of BubR1 onto kinetochores in prophase, before that of CENP-E[43], this raises the possibility that BubR1 is an adaptor that is at least partly responsible for targeting CENP-E to kinetochores. In some systems, this may be reciprocal, as *in vitro* establishment and maintenance of an activated checkpoint in *Xenopus* extracts requires the continued presence of CENP-E (A.A., J. A. Kahana and D.W.C., unpublished observations). In this model (see Fig. 7c), initial attachment of kinetochore-bound CENP-E to spindle microtubules affects checkpoint signalling both directly, through interaction with BubR1 (altering the activity and/or kinetochore affinity of BubR1) and indirectly, by promoting development of a stable bundle of kinetochore fibres and tension-dependent stretching of the kinetochores of bi-orientated chromosome pairs. In the mammalian context, the fact that the signal can be at least partially silenced on aligned chromosomes when CENP-E levels are diminished (as shown by reduced binding of Mad2 or BubR1) indicates either that very few molecules of CENP-E required or, more probably, that there is some redundancy in components that participate in silencing BubR1 signalling. □

Methods

Cell culture.

HeLa cells, from the American Type Culture Collection (Rockville, Maryland) were maintained as subconfluent monolayers in RPMI1640 media (Gibco/BRL) with 10% FCS (Gemini Bio-Products, Calabasas, California) and 100 U ml^{-1} penicillin plus 100 g ml^{-1} streptomycin (Gibco/BRL).

Transfection of antisense oligonucleotides.

HeLa cells were grown to near-confluence on 150-mm^2 culture flasks at 37 °C with 5% CO_2; mitotic cells were selected by mitotic shake-off. Two hours after replating into six-well plates with or without coverslips, cells (now in early G1) were transfected according to the manufacturer's protocol with 2 µg ml^{-1} lipofectin or lipofectamine (Gibco/BRL) premixed with various oligonucleotides. Several regions of CENP-E messenger RNA were selected for targeting with antisense oligonucleotides. Among various oligonucleotides, the one targeted to the sequence 5′-TTCAGCCTGATAGGATGGCGGAGG was found to be effective; a scrambled sequence of this oligonucleotide was used as a control. All oligonucleotides were used as phosphothoirates to increase the stability of the nucleotides[44]. Transfection efficiency was assessed by fluorescence microscopy to follow the uptake of fluorescein-isothiocyanate-labelled oligonucleotides. Transfection efficiency was typically 85±4%.

After various time intervals, cells were either fixed for immunofluorescence microscopy (see below), or were collected with a rubber policeman, centrifuged and solubilized in RIPA buffer (25 mM Tris–HCl pH7.5, 5 mM EDTA, 0.5% SDS and 1% deoxycholate). Extracts were then sonicated and centrifuged to remove residual insoluble materials. Before electrophoresis, an appropriate amount of extract was diluted with a fourfold volume of sample buffer and boiled for 2 min. To analyse protein-accumulation profiles across the subsequent cell cycle, equal proportions of each sample were subjected to SDS–PAGE. Proteins were then transferred onto a nitrocellulose membrane (MSI, Westborough, Massachusetts) and incubated with antibodies against CENP-E, Mad2, β-tubulin and cyclin B, and then with ^{125}I-labelled protein A. Immunoreactive signals were visualized by autoradiography on Kodak BioMAX MS film for 6–8 h at –80 °C, using an intensifying screen. Signals were quantified by phosphorimaging using ImageQuant Software (Molecular Dynamics, Sunnyvale, California).

Antibodies.

Antibodies against part of the coiled-coil domain of CENP-E (amino acids 955–1,571) were raised in rabbits as described[45]. Anti-Mad2 antibody was a gift from Y. Li (Memorial-Sloan Kettering Cancer Center, New York). Anti-tubulin antibody (YL1/2) was a gift from J. Kilmartin (MRC, Cambridge, UK). Antibody against cytoplasmic dynein was a gift from E. Vaisberg (University of Colorado, Boulder, Colorado). Anti-CENP-F antibodies were from T. Yen (Fox Chase Cancer Center, Philadelphia, Pennsylvania). Myc–BubR1 construct was from F. McKeon (Harvard University, Boston, Massachusetts). Mouse monoclonal antibody 9E10.2 against the c-Myc epitope was from ATCC (UCSF, San Francisco, California).

Immunofluorescence microscopy.

For immunofluorescence, cells synchronized by mitotic shake-off were seeded onto sterile, acid-treated 18-mm coverslips in 6-well plates (Corning Glass Works, Corning, New York). Two hours after replating, synchronized HeLa cells were transfected with 2 µg ml^{-1} lipofectamine premixed with various oligonucleotides as described above. At various times after transfection with antisense or scrambled (control) oligonucleotides, cells were rinsed for 1 min with PHEM buffer (100 mM PIPES, 20 mM HEPES pH6.9, 5 mM EGTA, 2 mM $MgCl_2$ and 4 M glycerol), permeabilized for 1 min with PHEM plus 0.1% Triton X-100 as described[32]. Extracted cells were then fixed in freshly made 4% paraformaldehyde plus 0.05% glutaraldehyde in PHEM, and rinsed three times in PBS. Coverslips were blocked with 0.05% Tween-20 in PBS (TPBS) with 1% BSA (Sigma). Cells were incubated with various primary antibodies in an humidified chamber for 1 h and then washed three times in TPBS. To visualize microtubules simultaneously, cells were incubated with YL1/2 anti-tubulin antibody[46] in an humidified chamber for 1 h and then washed three times in TPBS. Rabbit polyclonal antibodies bound to CENP-E and CENP-F were visualized using rhodamine-conjugated goat anti-rabbit immunoglobulin G (IgG), and binding of anti-tubulin antibody was visualized using fluorescein-conjugated goat anti-rat IgG. DNA was stained with DAPI (Sigma). Slides were examined with a Zeiss axiophot fluorescence microscope and images were collected and analyzed with MetaMorph software (Universal Imaging).

Deconvolution microscopy.

Deconvolution images were collected using a Deltavision wide-field deconvolution microscope system built on an Olympus IX-70 inverted microscope base. For imaging, a ×100 1.35 NA lens was used and optical sections were taken at intervals of 0.2 µm. Images were processed using DeltaVision Softworx

software on a Sun Octane workstation. Images for display were generated by projecting the sum of the optical sections using the maximum-intensity method. For presentation of details of the internal spindle in Fig. 3, projection images were constructed from a 1-μm section within the cell.

Measurement of interkinetochore distance.

The distance between sister kinetochores was measured using Metamorph software (Universal Imaging), ACA-marked centromeres and a Zeiss axiophot fluorescent microscope calibrated with a stage micrometer. When suitable kinetochore pairs were identified, the image was enlarged threefold to facilitate accurate placement of a computer-generated cursor over the centre of each kinetochore. Only sister kinetochores that were in the same focal plane were measured.

Transient transfection and immunoprecipitation.

HeLa cells were grown to ~50% confluency in DMEM with 10% FBS at 37 °C in 5% CO_2. Cells were then transfected with Myc–BubR1 by lipofectamine, according to manufacturer's protocol (Gibco/BRL). Mitotic cells were collected 24 h after transfection by treatment with 100 ng ml^{-1} nocodazole for 18 h, and proteins were solubilized in lysis buffer (50 mM HEPES pH 7.4, 150 mM NaCl, 2 mM EGTA, 0.1% Triton X-100, 1 mM phenylmethylsulphonyl fluoride, 10 g ml^{-1} leupeptin and 10 g ml^{-1} pepstatin A). Lysates were clarified by centrifugation at 16,000*g* for 10 min at 4 °C. Myc-tagged fusion proteins were incubated with anti-Myc monoclonal antibody 9E10 (ref. 47) bound to protein-A beads (Bio-Rad).Beads were washed five times with lysis buffer and then boiled in SDS–PAGE sample buffer for 2 min. After SDS–PAGE, proteins were transferred to a nitrocellulose membrane. The nitrocellulose was divided into four strips and incubated with antibodies against CENP-F, CENP-E, the Myc epitope and Mad2, respectively, and then with ^{125}I-labelled protein A. Immunoreactive signals were visualized by autoradiography on Kodak BioMAX film for 6–8 h at –80 °C, using an intensifying screen.

RECEIVED 19 JANUARY 2000; REVISED 4 MAY 2000; ACCEPTED 4 MAY 2000;
PUBLISHED 10 JULY 2000.

1. Brinkley, B. R. & Stubblefield, E. The fine structure of the kinetochore of a mammalian cell *in vitro*. *Chromosoma* **19,** 28–43 (1966).
2. Nicklas, R. B. The motor for poleward chromosome movement in anaphase is in or near the kinetochore. *J. Cell Biol.* **109,** 2245-2255 (1989).
3. Rieder, C. L. & Alexander, S. P. Kinetochores are transported poleward along a single astral microtubule during chromosome attachment to the spindle in newt lung cells. *J. Cell Biol.* **110,** 81–95 (1990).
4. Hyman, A. A. & Mitchison, T. J. Two different microtubule-based motor activities with opposite polarities in kinetochores. *Nature* **351,** 206–211 (1991).
5. Roos, U-P. Light and electron microscopy of rat kangaroo cells in mitosis. III. Patterns of chromosome behavior during prometaphase. *J. Cell Biol.* **54,** 363–385 (1976).
6. Bajer, A. S. Functional autonomy of monopolar spindle and evidence for oscillatory movement in mitosis. *J. Cell Biol.* **93,** 33–48 (1982).
7. Alexander, S. P. & Rieder, C. L. Chromosome motion during attachment to the vertebrate spindle: initial saltatory-like behavior of chromosomes and quantitative analysis of force production by nascent kinetochore fibers. *J. Cell Biol.* **113,** 805–815 (1991).
8. Skibbens, R. V., Skeen, V. P. & Salmon, E. D. Directional instability of kinetochore motility during chromosome congression and segregation in mitotic newt lung cells: a push-pull mechanism. *J. Cell Biol.* **122,** 859–875 (1993).
9. Khodjakov, A. & Rieder, C. L. Kinetochores moving away from their associated pole do not exert a significant pushing force on the chromosome. *J. Cell Biol.* **135,** 315–327 (1996).
10. Rieder, C. L., Cole, R. W., Khodjakov, A. & Sluder, G. The checkpoint delaying anaphase in response to chromosome monoorientation is mediated by an inhibitory signal produced by unattached kinetochores. *J. Cell Biol.* **130,** 941–948 (1995).
11. Li, R. & Murray, A. W. Feedback control of mitosis in budding yeast. *Cell* **66,** 519–531 (1991).
12. Hoyt, M. A., Totis, L. & Roberts, B. T. *S. cerevisiae* genes required for cell cycle arrest in response to loss of microtubule function. *Cell* **66,** 507–517 (1991).
13. Li, X. & Nicklas, R. B. Mitotic forces control a cell-cycle checkpoint. *Nature* **373,** 630–632 (1995).
14. Zhang, D. & Nicklas, R. B. 'Anaphase' and cytokinesis in the absence of chromosomes. *Nature* **382,** 466–468 (1996).
15. Chen, R. H., Waters, J. C., Salmon, E. D. & Murray, A. W. Association of spindle assembly checkpoint component XMAD2 with unattached kinetochores. *Science* **274,** 242–246 (1996).
16. Li, Y. & Benezra, R. Identification of a human mitotic checkpoint gene: hsMAD2. *Science* **274,** 246–248 (1996).
17. Taylor, S. S., Ha, E. & McKeon, F. The human homologue of Bub3 is required for kinetochore localization of Bub1 and a Mad3/Bub1-related protein kinase. *J. Cell Biol.* **142,** 1–11 (1998).
18. Martinez-Exposito, M. J., Kaplan, K. B., Copeland, J. & Sorger, P. K. Retention of the BUB3 checkpoint protein on lagging chromosomes. *Proc. Natl Acad. Sci. USA* **96,** 8493–8498 (1999).
19. Taylor, S. S. & McKeon, F. Kinetochore localization of murine Bub1 is required for normal mitotic timing and checkpoint response to spindle damage. *Cell* **89,** 727–735 (1997).
20. Chan, G. K. T., Jablonski, S. A., Sudakin, V., Hittle, J. C. & Yen, T. J. Human BUBR1 is a mitotic checkpoint kinase that monitors CENP-E functions and binds the cyclosome/APC. *J. Cell Biol.* **146,** 941–954 (1999).
21. Wood, K. W., Sakowicz, R., Goldstein, L. S. B. & Cleveland, D. W. CENP-E is a plus end-directed kinetochore motor required for metaphase chromosome alignment. *Cell* **91,** 357–366 (1997).
22. Brown, K. D., Coulson, R. M., Yen, T. J. & Cleveland, D. W. Cyclin-like accumulation and loss of the putative kinetochore motor CENP-E results from coupling continuous synthesis with specific degradation at the end of mitosis. *J. Cell Biol.* **125,** 1303–1312 (1994).
23. Lombillo, V. A., Nislow, C., Yen, T. J., Gelfand, V. I. & McIntosh, J. R. Antibodies to the kinesin motor domain and CENP-E inhibit microtubule depolymerization-dependent motion of chromosomes *in vitro*. *J. Cell Biol.* **128,** 107–115 (1995).
24. Yen, T. J. *et al.* CENP-E, a novel human centromere-associated protein required for progression from metaphase to anaphase. *EMBO J.* **10,** 1245–1254 (1991).
25. Duesbery, N. S. *et al.* CENP-E is an essential kinetochore motor in maturing oocytes and is masked during mos-dependent, cell cycle arrest at metaphase II. *Proc. Natl Acad. Sci. USA* **94,** 9165–9170 (1997).
26. Schaar, B. T., Chan, G. K. T., Maddox, P., Salmon, E. D. & Yen, T. J. CENP-E function at kinetochores is essential for chromosome alignment. *J. Cell Biol.* **139,** 1373–1382 (1997).
27. Chan, G. K. T., Schaar, B. T. & Yen, T. J. Characterization of the kinetochore binding domain of CENP-E reveals interactions with the kinetochore proteins CENP-F and hBUBR1. *J. Cell Biol.* **143,** 49–63 (1998).
28. Waters, J. C., Skibbens, R. V. & Salmon, E. D. Oscillating mitotic newt lung cell kinetochores are, on average, under tension and rarely push. *J. Cell Sci.* **109,** 2823–2831 (1996).
29. Steuer, E. R., Wordeman, L., Schroer, T. A. & Sheetz, M. P. Localization of cytoplasmic dynein to mitotic spindles and kinetochores. *Nature* **345,** 266–268 (1990).
30. Pfarr, C. M. *et al.* Cytoplasmic dynein is localized to kinetochores during mitosis. *Nature* **345,** 263–265 (1990).
31. Wordeman, L. & Mitchison, T. J. Identification and partial characterization of mitotic centromere-associated kinesin, a kinesin-related protein that associates with centromeres during mitosis. *J. Cell Biol.* **128,** 95–104 (1995).
32. Yao, X., Anderson, K. L. & Cleveland, D. W. The microtubule-dependent motor centromere-associated protein E (CENP-E) is an integral component of kinetochore corona fibers that link centromeres to spindle microtubules. *J. Cell Biol.* **139,** 435–447 (1997).
33. Rieder, C. L. The structure of the cold-stable kinetochore fiber in metaphase PtK 1 cells. *Chromosoma* **84,** 145–158 (1981).
34. Cassimeris, L., Rieder, C. L., Rupp, G. & Salmon, E. D. Stability of microtubule attachment to metaphase kinetochores in PtK1 cells. *J. Cell Sci.* **96,** 9–15 (1990).
35. Starr, D. A., Williams, B. C., Hays, T. S. & Goldberg, M. L. ZW10 helps recruit dynactin and dynein to the kinetochore. *J. Cell Biol.* **142,** 763–774 (1998).
36. Merdes, A., Ramyar, K., Vechio, J. D. & Cleveland, D. W. A complex of NuMA and cytoplasmic dynein is essential for mitotic spindle assembly. *Cell* **87,** 447–458 (1996).
37. Merdes, A., Heald, R., Samejima, K., Earnshaw, W. C. & Cleveland, D. W. Formation of spindle poles by dynein/dynactin-dependent transport of NuMA. *J. Cell Biol.* (submitted).
38. Walczak, C. E., Mitchison, T. J. & Desai, A. XKCM1: a *Xenopus* kinesin-related protein that regulates microtubule dynamics during mitotic spindle assembly. *Cell* **84,** 37–47 (1996).
39. Desai, A., Verma, S., Mitchison, T. J. & Walczak, C. E. Kin I kinesins are microtubule-destabilizing enzymes. *Cell* **96,** 69–78 (1999).
40. Maney, T., Hunter, A. W., Wagenbach, M. & Wordeman, L. Mitotic centromere-associated kinesin is important for anaphase chromosome segregation. *J. Cell Biol.* **142,** 787–801 (1998).
41. Vaisberg, E. A., Koonce, M. P. & McIntosh, J. R. Cytoplasmic dynein plays a role in mammalian mitotic spindle formation. *J. Cell Biol.* **123,** 849–858 (1993).
42. Echeverri, C. J., Paschal, B. M., Vaughan, K. T. & Vallee, R. B. Molecular characterization of the 50-kD subunit of dynactin reveals function for the complex in chromosome alignment and spindle organization during mitosis. *J. Cell Biol.* **132,** 617–633 (1996).
43. Jablonski, S. A., Chan, G. K. T., Cooke, C. A., Earnshaw, W. C. & Yen, T. J. The hBUB1 and hBUBR1 kinases sequentially assemble onto kinetochores during prophase with hBUBR1 concentrating at the kinetochore plates in mitosis. *Chromosoma* **107,** 386–396 (1998).
44. Caceres, A. & Kosik, K. S. Inhibition of neurite polarity by tau antisense oligonucleotides in primary cerebellar neurons. *Nature* **343,** 461–463 (1990).
45. Brown, K. D., Wood, K. W. & Cleveland, D. W. The kinesin-like protein CENP-E is kinetochore-associated throughout poleward chromosome segregation during anaphase-A. *J. Cell Sci.* **109,** 961–969 (1996).
46. Kilmartin, J. V., Wright, B. & Milstein, C. Rat monoclonal antitubulin antibodies derived by using a new nonsecreting rat cell line. *J. Cell Biol.* **93,** 576–582 (1982).
47. Evan, G. I., Lewis, G. K., Ramsay, G. & Bishop, J. M. Isolation of monoclonal antibodies specific for human c-myc proto-oncogene product. *Mol. Cell Biol.* **5,** 3610–3616 (1985).
48. Fang, G., Yu, H. & Kirschner, M. W. The checkpoint protein MAD2 and the mitotic regulator CDC20 form a ternary complex with the anaphase-promoting complex to control anaphase initiation. *Genes Dev.* **12,** 1871–1883 (1998).

ACKNOWLEDGMENTS

This work was supported by a grant from the National Institute of Health (GM29513) to D.W.C. Salary support for D.W.C. is provided by the Ludwig Institute for Cancer Research. X.Y. was supported by postdoctoral fellowships from the Bank of America Giannini Foundation and the American Cancer Society (California Division), and by a Career Development Award from the Howard Hughes Medical Institute/University of Wisconsin.

Correspondence and requests for materials should be addressed to D.W.C.